

SUPPORTING INFORMATION:

We have compared our data to standard tunneling models in order to confirm that our single level picture is indeed the most suitable description for the experimental curves. Since the bias voltage V is comparable with the height of the tunneling barrier E_0 , Fowler-Nordheim tunneling might be expected to be an appropriate description for the process.¹ In this regime the current is given by

$$I \propto V^2 \exp\left(-\frac{4d\sqrt{2m}E_0^{3/2}}{3e\hbar V}\right),$$
 with d the distance between the electrodes and m the electron mass. This

dependence can be tested easily by plotting $\ln(I/V^2)$ vs. $1/V$, as shown in **Figure SI-1**.

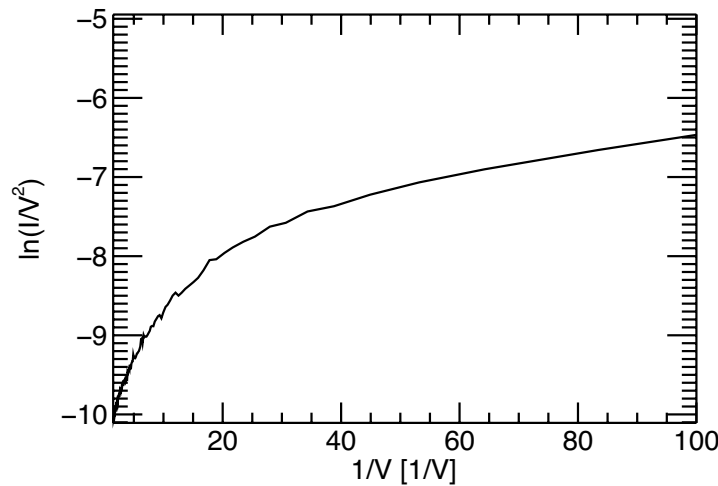


Figure SI-1. Fowler-Nordheim plot for the I - V curve shown in figure 1 measured for BNT.

It can be clearly seen that the experimental data deviate from the linear behavior. This fact indicates that the data cannot be described with this model regardless of the fit parameters chosen.

The Simmons model² is another alternative. This model leads to current levels on the order of 1 nA if we assume a contact area of approximately 1 nm^2 and a distance of about 1 nm. Larger contact areas can be excluded because we observe the typical single-atom-contact behavior when opening and closing the junctions. At smaller distances we observe linear I - V curves, consistent with direct tunneling between the two metallic contacts. Therefore this model does not lead to a satisfactory description of our data as well.

An additional strength of the single level tunneling model lies in its ability to describe with the same precision asymmetric I -Vs. A considerable percentage of the experimentally recorded I -Vs are asymmetric. The degree of asymmetry varies from species to species. The asymmetry is accounted for in the model in a very natural way by using different values for the coupling parameters to the left and the right electrode: $\Gamma_L \neq \Gamma_R$. In addition, we assume that the energy level appearing in eq 2 acquires a voltage dependence given by

$$E_0(V) = E_0 + \left(\frac{\Gamma_L - \Gamma_R}{\Gamma_L + \Gamma_R} \right) \frac{eV}{2} .$$

Here, $E_0(V)$ is the modified energy level and E_0 is the position of the level under symmetric conditions (or at zero bias). This modification accounts for the fact that the largest voltage drop is expected to occur at the interface with the weakest coupling. In particular, if the molecule is much more strongly coupled to one of the electrodes, this equation tells us that the energy level moves with the bias following the chemical potential of that electrode. As an example we show in **Figure SI-2** an I - V curve recorded on BNT with asymmetric coupling and a fit to the single level tunneling model with the parameters $\Gamma_L = 90$ meV, $\Gamma_R = 61$ meV, and $E_0 = 0.59$ eV. A detailed analysis of asymmetric I -Vs will be subject of a forthcoming publication.

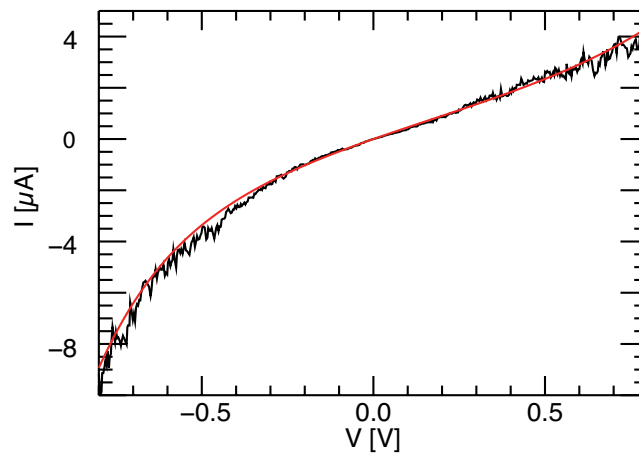


Figure SI-2. Asymmetric I - V (black) taken on BNT with a fit to the single level model assuming asymmetric coupling to the electrodes (red).

Turning now to the theory, for BNT we have found a binding geometry for which the transport is dominated by more than a single level. This geometry is shown in **Figure SI-3** where one can see that the molecule binds to the gold electrodes via two Au-O bonds on each side. In this case, the transmission around the Fermi energy is dominated by the contributions of the LUMO and LUMO+1 of the isolated molecule. Notice also that the low-bias conductance is very high and the I - V curve is rather linear up to 0.5 V (see left inset of Figure SI-3), which resembles the experimental results. This suggests that in this case the use of the single level model might not be justified in general for this molecule.

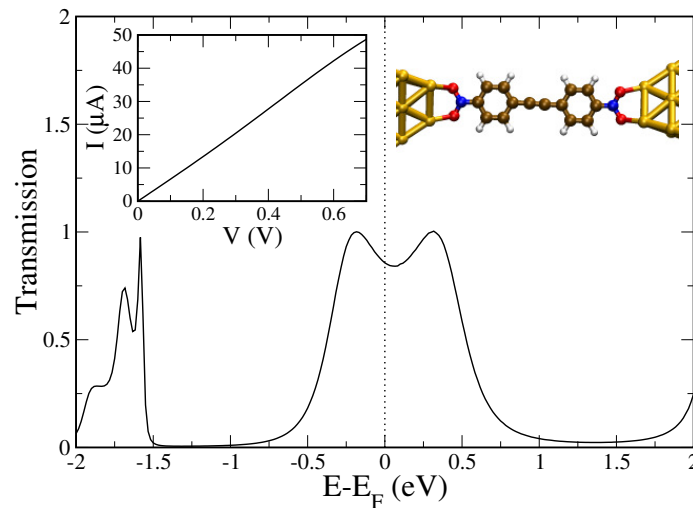


Figure SI-3. Zero-bias transmission as a function of energy for a BNT junction with two Au-O bonds on each side (see right inset). The inset on the left shows the corresponding I - V characteristics obtained by simply integrating the zero-bias transmission, see eq 1.

Another issue that we have addressed is the dependence of Γ and E_0 upon stretching of the contacts. In order to clarify this issue we have performed DFT simulations of the stretching process for all the molecules in top binding geometries. For BNT, the trans structure was chosen. The simulations were done by starting with the equilibrium geometries of Figure 3 (or slightly compressed ones), and then the gold electrodes were separated step-wise by a distance of 0.4 Å per step. In every step the central part of the geometries was re-optimized including the molecules and the last 4 gold atoms in both electrodes. As an example, we show in **Figure SI-4** geometries of the BTT contact in different stages of the

elongation process and their corresponding transmission curves. In every step we also computed the total energy of the contact, the force required to breaking the contact and we extracted both Γ and E_0 from the analysis of the transmission curves. The results for the four molecules are summarized in **Figure SI-5**. In this figure one can see that we do not find strong variations of the coupling strength Γ during the stretching process. For instance, for BTT, where the contact has been elongated in total by more than 2 Å, Γ varies from 110 meV in for the equilibrium geometry to 40 meV when the contact breaks. These values are within the range of the experimental results (see Figure 2). It is interesting to notice that for this particular geometry the conductance for BTT and BAT increases upon stretching until the contacts break. This is due to the fact that the HOMO moves closer to the Fermi energy, which over-compensates the reduction of the broadening of the molecular orbital (see Figure SI-4). An increase in conductance upon stretching has been predicted in other theoretical studies^{3,4} and it is considered as a signature of coherent transport. We show below that it is possible for the thiol group to find evolutions where the increase of the conductance is accompanied by an increase in Γ , similar to what the experiments suggest (see Figure 2).

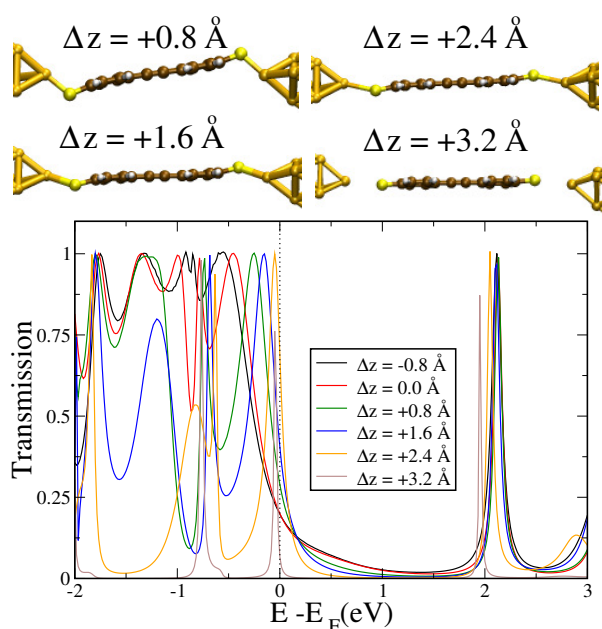


Figure SI-4. Transmission as a function of energy at different stages of the stretching process of a BTT junction where the molecule was initially in a top position. Here, Δz indicates the elongation as

measured with respect to the equilibrium junction and some snapshots of the evolution of the junction are shown in the upper part of this graph.

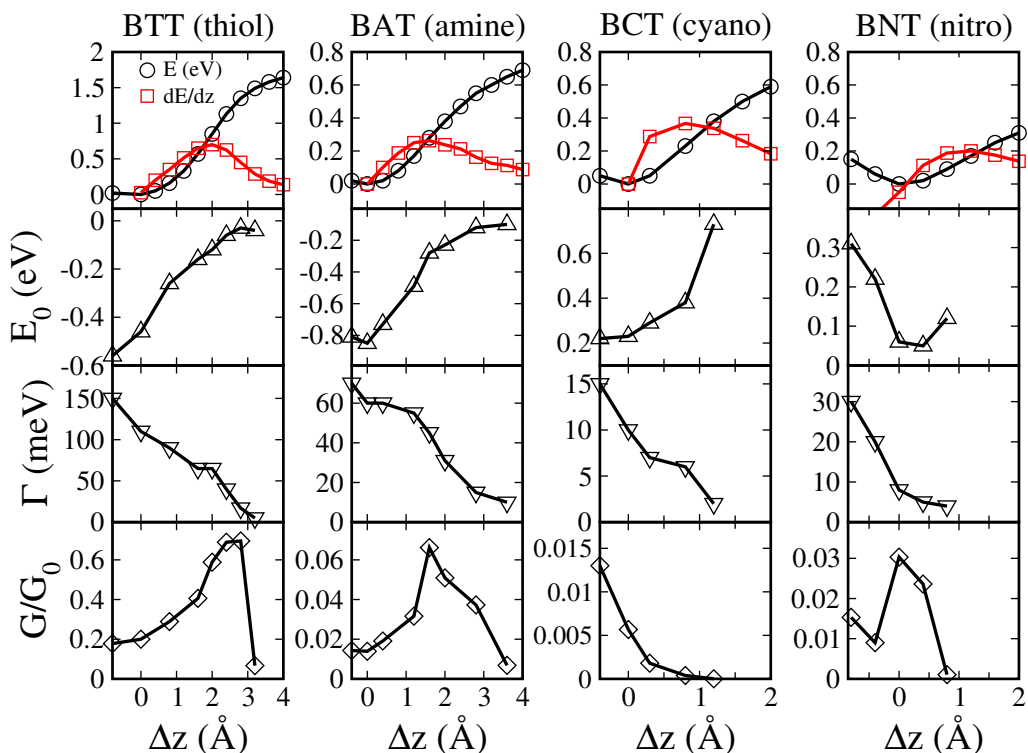


Figure SI-5. Total energy, force, E_0 , Γ and conductance as a function of the elongation of junctions (Δz) with the four molecules in a top binding geometry.

On the other hand, one might be tempted to think that there is direct relation between the metal-molecule bond strength (or the junction binding energy) and the broadening Γ and in turn with the conductance. Our analysis shows however that this naïve idea is in general not correct. This is especially clear in the cases of BCT and BNT where the LUMO dominates the transport, but it plays practically no role in the binding of the molecule to the metal. For practical purposes, we define the junction binding energies as the absolute value of the difference between the energy of a given geometry and the asymptotic value obtained at very large distances when the contacts are completely broken (due to the symmetry of these contacts, they break into three separate pieces). For the most stable geometries in Figure SI-5 we obtain the following binding energies: 1.83 eV for BTT, 0.98 eV for BCT, 0.86 eV for BAT and 0.73 eV for BNT. Thus, as one can see in Figure SI-5, neither the corresponding values of the coupling parameter Γ nor those of the linear conductance follow the same trend as the binding energies.

Another interesting issue is the relation between the bond strength and the distance over which a junction can be stretched (i.e. the length of the conductance plateaus). Defining this distance as the elongation needed to reach the maximum value of the force starting from the equilibrium geometries, we obtain the following lengths: 2 Å for BTT, 1.6 Å for BAT, 1.2 Å for BNT and 0.8 Å for BCT. Again, notice that there is not a simple correlation between the length of the plateaus and the binding energies (see previous paragraph). One could think naïvely that e.g. the cyano-mediated binding is much weaker than the amine one, since it breaks at shorter distances. However, the binding energy and the force are higher for BCT. This indicates that the cyano-gold bond is actually stronger than amine-gold bond. On the other hand, let us mention that recent experiments have shown indeed longer conductance plateaus with S linkage than with NH₂ termination,⁵ in agreement with our calculations. Moreover, in accordance with Ref. 19 of the main text, we found a less abrupt conductance drop for BAT than for BTT, due to a smaller gold retraction in BAT after rupture.

We also want to point out that more complex evolutions of the values of Γ upon stretching than the ones shown in Figure SI-5 are possible. For example, stretching BTT in the hollow binding geometry leads to a different behavior, as one can see **Figure SI-6**. After elongating the contact by 0.8 Å, the S atom moves to a top position on one of the three top atoms. This is visible as a sudden increase of the value of Γ values. Notice also that in the range between 0.8 and 2.5 Å the increase of the conductance is followed by an increase in Γ , as opposed to the example of the top position shown in Figure SI-5, and more in accordance with the experimental findings (see Figure 2).

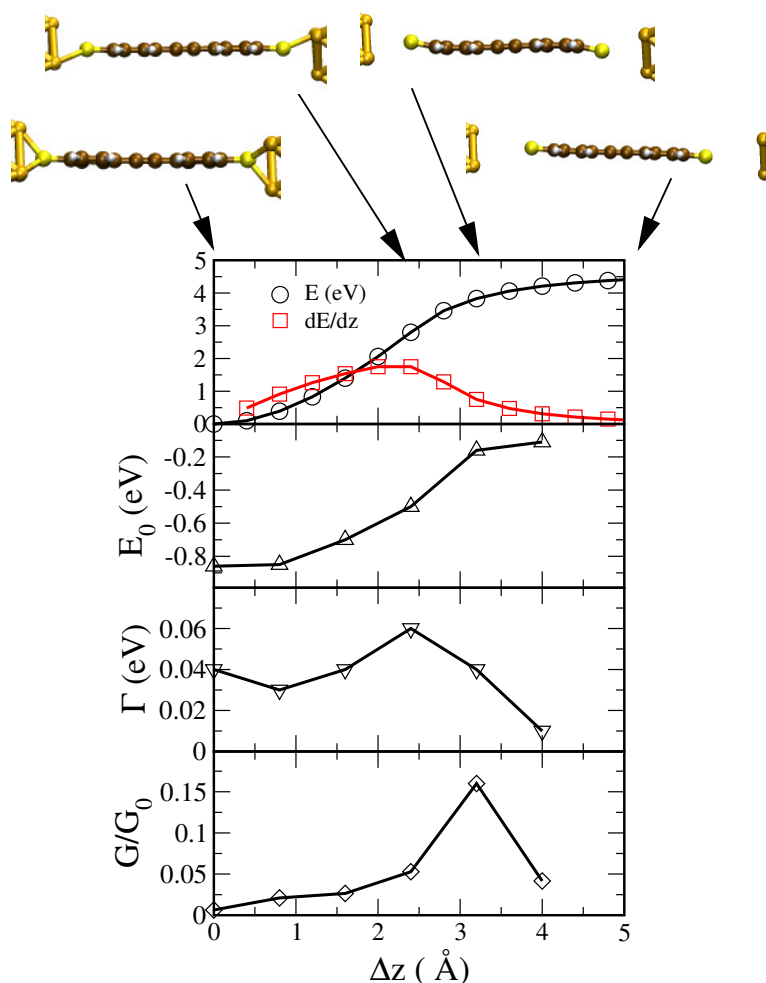


Figure SI-6. Dependence of relative total energy, pulling force, E_0 measured with respect to the Fermi energy, Γ and conductance on the elongation for BTT in hollow binding geometry. In the upper part of the graph we show several geometries obtained at different stages of the stretching process.

[1] W. Wang, T. Lee, and M. A. Reed, *Phys. Rev. B* **2003**, *68*, 035416.

[2] S. A. G. Vrouwe, E. van der Giessen, S. J. van der Molen, D. Dulic, M. L. Trouwborst, and B. J. van Wees, *Phys. Rev. B* **2005**, *71*, 35313.

[3] R. C. Hoft, M. J. Ford, M. B. Cortie, *Chem. Phys. Lett.* **2006**, *429*, 503.

[4] I. S. Kristensen, D. J. Mowbray, K. S. Thygesen, K. W. Jacobsen, *J. Phys.: Condens. Matter* **2008**, *20*, 374101.

[5] Y. S. Park, A. C. Whalley, M. Kamenetska, M. L. Steigerwald, M. S. Hybertsen, C. Nuckolls, L. Venkataraman, *J. Am. Chem. Soc.* **2007**, *129*, 15768.